



# Manipulator Differential Kinematics

## Part I: Kinematics, Velocity, and Applications

By Jesse Haviland and Peter Corke

**M**anipulator kinematics is concerned with the motion of each link within a manipulator without considering mass or force. In this article, which is the first in a two-part tutorial, we provide an introduction to modelling manipulator kinematics using the elementary transform sequence (ETS). Then we formulate the first-order differential kinematics, which leads to the manipulator Jacobian, which is the basis for velocity control and inverse kinematics. We describe essential classical techniques which rely on the manipulator Jacobian before exhibiting some contemporary applications. Part II of this tutorial provides a formulation of second and higher-order differential kinematics, introduces the manipulator Hessian, and illustrates advanced techniques, some of which improve the performance of techniques demonstrated in Part I.

We have provided Jupyter Notebooks to accompany

each section within this tutorial. The Notebooks are written in Python code and use the Robotics Toolbox for Python, and the Swift Simulator [1] to provide examples and implementations of algorithms. While not absolutely essential, for the most engaging and informative experience, we recommend working through the Jupyter Notebooks while reading this article. The Notebooks and setup instructions can be accessed at [github.com/jhav1/dkt](https://github.com/jhav1/dkt).

A serial-link manipulator, which we refer to as a manipulator, is the formal name for a robot that comprises a chain of rigid links and joints, it may contain branches, but it can not have closed loops. Each joint provides one degree of freedom, which may be a prismatic joint providing translational freedom or a revolute joint providing rotational freedom. The base frame of a manipulator represents the reference frame of the first link in the chain,

while the last link is known as the end-effector.

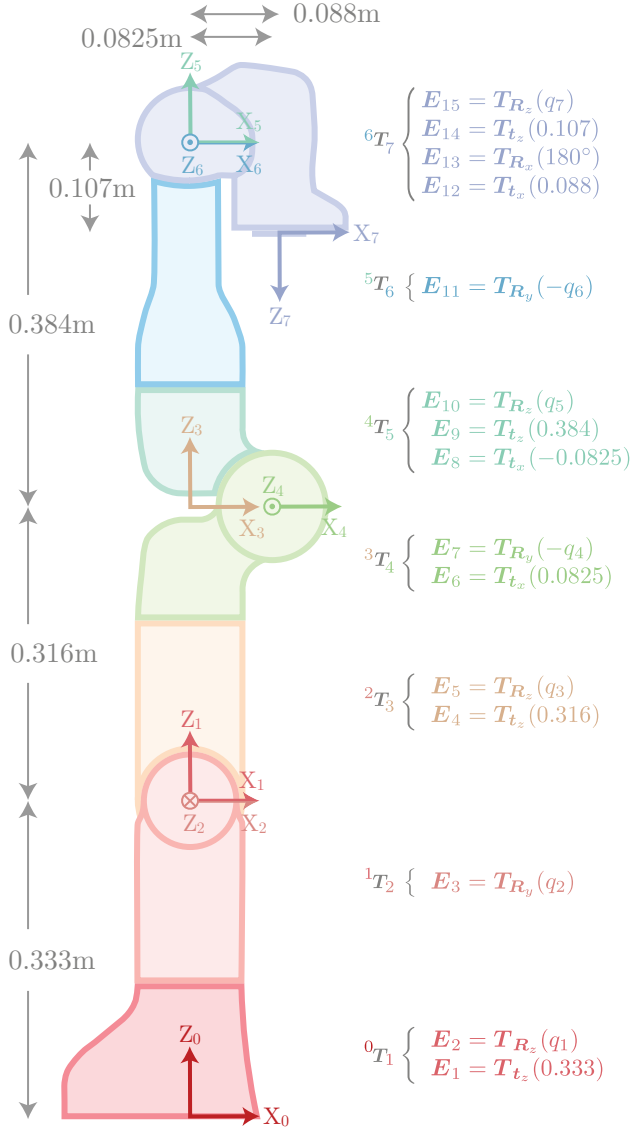


**Figure 1.** The Elementary Transform Sequence of the 7 degree-of-freedom Franka-Emika Panda serial-link manipulator in its zero-angle configurations.  $\mathbf{E}_i$  represents an elementary transform while  ${}^a\xi_b$  represents the pose of link frame  $b$  in the reference frame of link  $a$ .

Manipulator kinematics is an essential area of study and provides the foundation for manipulator control. The motion of each joint within a manipulator modifies the pose of all subsequent links, and ultimately the pose of the end-effector.

The elementary transform sequence (ETS), introduced in [2], provides a universal method for describing the kinematics of any manipulator. This intuitive and systematic approach can be applied with a simple *walk through* procedure. The resulting sequence comprises a number of elementary transforms – translations and rotations – from the base frame to the robot’s end-effector.

$$\mathbf{T}_{t_x}(\eta) = \begin{pmatrix} 1 & 0 & 0 & \eta \\ 0 & 1 & 0 & 0 \\ 0 & 0 & 1 & 0 \\ 0 & 0 & 0 & 1 \end{pmatrix}$$

$$\mathbf{T}_{t_y}(\eta) = \begin{pmatrix} 1 & 0 & 0 & 0 \\ 0 & 1 & 0 & \eta \\ 0 & 0 & 1 & 0 \\ 0 & 0 & 0 & 1 \end{pmatrix}$$

$$\mathbf{T}_{t_z}(\eta) = \begin{pmatrix} 1 & 0 & 0 & 0 \\ 0 & 1 & 0 & 0 \\ 0 & 0 & 1 & \eta \\ 0 & 0 & 0 & 1 \end{pmatrix}$$

$$\mathbf{T}_{R_x}(\eta) = \begin{pmatrix} 1 & 0 & 0 & 0 \\ 0 & \cos(\eta) & -\sin(\eta) & 0 \\ 0 & \sin(\eta) & \cos(\eta) & 0 \\ 0 & 0 & 0 & 1 \end{pmatrix}$$

$$\mathbf{T}_{R_y}(\eta) = \begin{pmatrix} \cos(\eta) & 0 & \sin(\eta) & 0 \\ 0 & 1 & 0 & 0 \\ -\sin(\eta) & 0 & \cos(\eta) & 0 \\ 0 & 0 & 0 & 0 \end{pmatrix}$$

$$\mathbf{T}_{R_z}(\eta) = \begin{pmatrix} \cos(\eta) & -\sin(\eta) & 0 & 0 \\ \sin(\eta) & \cos(\eta) & 0 & 0 \\ 0 & 0 & 1 & 0 \\ 0 & 0 & 0 & 1 \end{pmatrix}$$

**Figure 2.** The six elementary transforms  $\mathbf{E} \in \mathbf{SE}(3)$  from (2) which are the building blocks for ETS notation. Each homogeneous transformation matrix represents a translation along, or a rotation about, a single axis which is parameterized by  $\eta$  as defined in (3) and (4)

An example of an ETS is displayed in Figure 1 for the Franka-Emika Panda in its zero-angle configuration.

The ETS is conceptually easy to grasp, since it avoids the frame assignment constraints of Denavit and Hartenberg (DH) notation [3], and allows joint rotation or translation about or along any axis.

We use the notation of [4] where  $\{a\}$  denotes a coordinate frame, and  ${}^a\mathbf{T}_b$  is a relative pose or rigid-body transformation of  $\{b\}$  with respect to  $\{a\}$ .

## Forward Kinematics

The forward kinematics is the first and most fundamental relationship between the link geometry and robot configuration.

The forward kinematics of a manipulator provides a non-linear mapping

$${}^0\mathbf{T}_e(t) = \mathcal{K}(\mathbf{q}(t))$$

between the joint space and Cartesian task space, where  $\mathbf{q}(t) = (q_1(t), q_2(t), \dots, q_n(t)) \in \mathbb{R}^n$  is the vector of joint generalised coordinates,  $n$  is the number of joints, and  ${}^0\mathbf{T}_e \in \mathbf{SE}(3)$  is a homogeneous transformation matrix representing the pose of the robot's end-effector in the world-coordinate frame. The ETS model defines  $\mathcal{K}(\cdot)$  as the product of  $M$  elementary transforms  $\mathbf{E}_i \in \mathbf{SE}(3)$

$$\begin{aligned} {}^0\mathbf{T}_e(t) &= \mathbf{E}_1(\eta_1) \mathbf{E}_2(\eta_2) \dots \mathbf{E}_M(\eta_M) \\ &= \prod_{i=1}^M \mathbf{E}_i(\eta_i). \end{aligned} \quad (1)$$

Each of the elementary transforms  $\mathbf{E}_i$  can be a pure translation along, or a pure rotation about the local x-, y-, or z-axis by an amount  $\eta_i$ . Explicitly, each transform is one of the following

$$\mathbf{E}_i = \begin{cases} \mathbf{T}_{t_x}(\eta_i) \\ \mathbf{T}_{t_y}(\eta_i) \\ \mathbf{T}_{t_z}(\eta_i) \\ \mathbf{R}_{R_x}(\eta_i) \\ \mathbf{R}_{R_y}(\eta_i) \\ \mathbf{R}_{R_z}(\eta_i) \end{cases} \quad (2)$$

where each of the matrices are displayed in Figure 2 and the parameter  $\eta_i$  is either a constant  $c_i$  (translational offset or rotation) or a joint variable  $q_j(t)$

$$\eta_i = \begin{cases} c_i \\ q_j(t) \end{cases} \quad (3)$$

The figure shows two mappings. On the left, a vector  $\mathbf{s} = \begin{bmatrix} s_1 \\ s_2 \\ s_3 \end{bmatrix}$  is mapped to a skew symmetric matrix  $\mathbf{S} = [\mathbf{s}]_{\times} = \begin{bmatrix} 0 & -s_3 & s_2 \\ s_3 & 0 & -s_1 \\ -s_2 & s_1 & 0 \end{bmatrix}$ . On the right, a vector  $\hat{\mathbf{s}} = \begin{bmatrix} s_1 \\ s_2 \\ s_3 \\ s_4 \\ s_5 \\ s_6 \end{bmatrix}$  is mapped to an augmented skew symmetric matrix  $\hat{\mathbf{S}} = [\hat{\mathbf{s}}] = \begin{bmatrix} 0 & -s_6 & s_5 & s_1 \\ s_6 & 0 & -s_4 & s_2 \\ -s_5 & s_4 & 0 & s_3 \\ 0 & 0 & 0 & 0 \end{bmatrix}$ .

**Figure 3.** Shown on the left is a vector  $\mathbf{s} \in \mathbb{R}^3$  along with its corresponding skew symmetric matrix  $\mathbf{S} \in \mathfrak{so}(3) \subset \mathbb{R}^{3 \times 3}$ . Shown on the right is a vector  $\hat{\mathbf{s}} \in \mathbb{R}^6$  along with its corresponding augmented skew symmetric matrix  $\hat{\mathbf{S}} \in \mathfrak{se}(3) \subset \mathbb{R}^{4 \times 4}$ . The skew functions  $[\cdot]_{\times} : \mathbb{R}^3 \mapsto \mathfrak{so}(3)$  maps a vector to a skew symmetric matrix, and  $[\cdot] : \mathbb{R}^6 \mapsto \mathfrak{se}(3)$  maps a vector to an augmented skew symmetric matrix. The inverse skew functions  $\vee_{\times}(\cdot) : \mathfrak{so}(3) \mapsto \mathbb{R}^3$  maps a skew symmetric matrix to a vector and  $\vee(\cdot) : \mathfrak{se}(3) \mapsto \mathbb{R}^6$  maps an augmented skew symmetric matrix to a vector.

and the joint variable is

$$q_j(t) = \begin{cases} \theta_j(t) & \text{for a revolute joint} \\ d_j(t) & \text{for a prismatic joint} \end{cases} \quad (4)$$

where  $\theta_j(t)$  represents a joint angle, and  $d_j(t)$  represents a joint translation.

An ETS description does not require intermediate link frames, but it does not preclude their introduction. The convention we adopt is to place the  $j^{\text{th}}$  frame immediately after the ETS term related to  $q_j$ , as shown in Figure 1. The relative transform between link frames  $a$  and  $b$  is simply a subset of the ETS

$${}^a\mathbf{T}_b = \prod_{i=\mu(a)}^{\mu(b)} \mathbf{E}_i(\eta_i) \quad (5)$$

where the function  $\mu(j)$  returns the index of the term in the ETS expression, (1) in this case, which is a function of  $q_j$ . For example, from Figure 1, for joint variable  $j = 5$ ,  $\mu(j) = 10$ .

## Deriving the Manipulator Jacobian

### First Derivative of a Pose

Now consider the end-effector pose, which is a function of the joint coordinates given by (1). Its derivative with respect to time is

$$\dot{\mathbf{T}} = \frac{d\mathbf{T}}{dt} = \frac{\partial \mathbf{T}}{\partial q_1} \dot{q}_1 + \dots + \frac{\partial \mathbf{T}}{\partial q_n} \dot{q}_n \in \mathbb{R}^{4 \times 4} \quad (6)$$

where each  $\frac{\partial \mathbf{T}}{\partial q_i} \in \mathbb{R}^{4 \times 4}$ .

The information in  $\mathbf{T}$  is non-minimal, and redundant, as is the information in  $\dot{\mathbf{T}}$ . We can write these respectively as

$$\mathbf{T} = \begin{pmatrix} \mathbf{R} & \mathbf{t} \\ 0 & 1 \end{pmatrix}, \quad \dot{\mathbf{T}} = \begin{pmatrix} \dot{\mathbf{R}} & \dot{\mathbf{t}} \\ 0 & 0 \end{pmatrix} \quad (7)$$

where  $\mathbf{R} \in \mathbf{SO}(3)$ ,  $\dot{\mathbf{R}} \in \mathbb{R}^{3 \times 3}$ , and  $\mathbf{t}, \dot{\mathbf{t}} \in \mathbb{R}^3$ .

We will write the partial derivative in partitioned form as

$$\frac{\partial \mathbf{T}}{\partial q_j} = \begin{pmatrix} \mathbf{J}_{R_j} & \mathbf{J}_{t_j} \\ 0 & 0 \end{pmatrix} \quad (8)$$

where  $\mathbf{J}_{R_j} \in \mathbb{R}^{3 \times 3}$  and  $\mathbf{J}_{t_j} \in \mathbb{R}^{3 \times 1}$ , and then rewrite (6) as

$$\begin{pmatrix} \dot{\mathbf{R}} & \dot{\mathbf{t}} \\ 0 & 0 \end{pmatrix} = \begin{pmatrix} \mathbf{J}_{R_1} & \mathbf{J}_{t_1} \\ 0 & 0 \end{pmatrix} \dot{q}_1 + \cdots + \begin{pmatrix} \mathbf{J}_{R_n} & \mathbf{J}_{t_n} \\ 0 & 0 \end{pmatrix} \dot{q}_n$$

and write a matrix equation for each non-zero partition

$$\dot{\mathbf{R}} = \mathbf{J}_{R_1} \dot{q}_1 + \cdots + \mathbf{J}_{R_n} \dot{q}_n \quad (9)$$

$$\dot{\mathbf{t}} = \mathbf{J}_{t_1} \dot{q}_1 + \cdots + \mathbf{J}_{t_n} \dot{q}_n \quad (10)$$

where each term represents the contribution to end-effector velocity due to motion of the corresponding joint.

Taking (10) first, we can simply write

$$\begin{aligned} \dot{\mathbf{t}} &= (\mathbf{J}_{t_1} \quad \cdots \quad \mathbf{J}_{t_n}) \begin{pmatrix} \dot{q}_1 \\ \vdots \\ \dot{q}_n \end{pmatrix} \\ &= \mathbf{J}_\nu(\mathbf{q}) \dot{\mathbf{q}} \end{aligned} \quad (11)$$

where  $\mathbf{J}_\nu(\mathbf{q}) \in \mathbb{R}^{3 \times n}$  is the translational part of the manipulator Jacobian matrix.

Rotation rate is slightly more complex, but using the identity  $\dot{\mathbf{R}} = [\boldsymbol{\omega}]_\times \mathbf{R}$  where  $\boldsymbol{\omega} \in \mathbb{R}^3$  is the angular velocity, and  $[\boldsymbol{\omega}]_\times \in \mathfrak{so}(3)$  is a skew-symmetric matrix, we can rewrite (9) as

$$[\boldsymbol{\omega}]_\times \mathbf{R} = \mathbf{J}_{R_1} \dot{q}_1 + \cdots + \mathbf{J}_{R_n} \dot{q}_n \quad (12)$$

and rearrange to

$$[\boldsymbol{\omega}]_\times = (\mathbf{J}_{R_1} \mathbf{R}^\top) \dot{q}_1 + \cdots + (\mathbf{J}_{R_n} \mathbf{R}^\top) \dot{q}_n \in \mathfrak{so}(3).$$

This  $3 \times 3$  matrix equation therefore has only 3 unique equations so applying the inverse skew operator to both sides we have

$$\begin{aligned} \boldsymbol{\omega} &= \vee_\times (\mathbf{J}_{R_1} \mathbf{R}^\top) \dot{q}_1 + \cdots + \vee_\times (\mathbf{J}_{R_n} \mathbf{R}^\top) \dot{q}_n \\ &= \left( \vee_\times (\mathbf{J}_{R_1} \mathbf{R}^\top) \quad \cdots \quad \vee_\times (\mathbf{J}_{R_n} \mathbf{R}^\top) \right) \begin{pmatrix} \dot{q}_1 \\ \vdots \\ \dot{q}_n \end{pmatrix} \\ &= \mathbf{J}_\omega(\mathbf{q}) \dot{\mathbf{q}} \end{aligned} \quad (13)$$

where  $\mathbf{J}_\omega(\mathbf{q}) \in \mathbb{R}^{3 \times n}$  is the rotational part of the manipulator Jacobian.

Combining (11) and (13) we can write

$${}^0 \boldsymbol{\nu} = \begin{pmatrix} \mathbf{v} \\ \boldsymbol{\omega} \end{pmatrix} = \begin{pmatrix} \mathbf{J}_\nu(\mathbf{q}) \\ \mathbf{J}_\omega(\mathbf{q}) \end{pmatrix} \dot{\mathbf{q}} \quad (14)$$

which expresses end-effector spatial velocity  ${}^0 \boldsymbol{\nu} = (v_x, v_y, v_z, \omega_x, \omega_y, \omega_z)$  in the world frame in terms of joint velocity and

$${}^0 \mathbf{J}(\mathbf{q}) = \begin{pmatrix} \mathbf{J}_\nu(\mathbf{q}) \\ \mathbf{J}_\omega(\mathbf{q}) \end{pmatrix} \in \mathbb{R}^{6 \times n} \quad (15)$$

is the manipulator Jacobian matrix expressed in the world-coordinate frame. The Jacobian expressed in the end-effector frame is

$${}^e \mathbf{J}(\mathbf{q}) = \begin{pmatrix} {}^0 \mathbf{R}_e^\top & \mathbf{0} \\ \mathbf{0} & {}^0 \mathbf{R}_e^\top \end{pmatrix} {}^0 \mathbf{J}(\mathbf{q}) \quad (16)$$

where  ${}^0 \mathbf{R}_e$  is a rotation matrix representing the orientation of the end-effector in the world frame.

Combining (14) and (15) we write

$${}^0 \boldsymbol{\nu} = {}^0 \mathbf{J}(\mathbf{q}) \dot{\mathbf{q}} \quad (17)$$

which provides the derivative of the left side of (1). However, in order to compute (17), we need to first compute (8), that is  $\frac{\partial \mathbf{T}}{\partial q_j}$ .

## First Derivative of an Elementary Transform

Before differentiating the ETS to find the manipulator Jacobian, it is useful to consider the derivative of a single Elementary Transform. In this section we use the skew and inverse skew operation as defined in Figure 3.

**Derivative of a Pure Rotation** The derivative of a rotation matrix with respect to the rotation angle  $\theta$  is required when considering a revolute joint and can be shown to be

$$\frac{d\mathbf{R}(\theta)}{d\theta} = [\hat{\boldsymbol{\omega}}]_\times \mathbf{R}(\theta(t)) \quad (18)$$

where the unit vector  $\hat{\boldsymbol{\omega}}$  is the joint rotation axis.

The rotation axis  $\hat{\boldsymbol{\omega}}$  can be recovered using the inverse skew operator

$$\hat{\boldsymbol{\omega}} = \vee_\times \left( \frac{d\mathbf{R}(\theta)}{d\theta} \mathbf{R}(\theta(t))^\top \right) \quad (19)$$

since  $\mathbf{R} \in \mathbf{SO}(3)$ , then  $\mathbf{R}^{-1} = \mathbf{R}^\top$ .

For an ETS, we only need to consider the elementary rotations  $\mathbf{R}_x$ ,  $\mathbf{R}_y$ , and  $\mathbf{R}_z$  which are embedded within  $\mathbf{SE}(3)$ , as  $\mathbf{T}_{\mathbf{R}_x}$ ,  $\mathbf{T}_{\mathbf{R}_y}$ , and  $\mathbf{T}_{\mathbf{R}_z}$  i.e. pure rotations with no translational component. We can show that the derivative of each elementary rotation with respect to a rota-

tion angle is

$$\frac{d\mathbf{T}_{\mathbf{R}_x}(\theta)}{d\theta} = \begin{pmatrix} 0 & 0 & 0 & 0 \\ 0 & 0 & -1 & 0 \\ 0 & 1 & 0 & 0 \\ 0 & 0 & 0 & 0 \end{pmatrix} \mathbf{T}_{\mathbf{R}_x}(\theta) = [\hat{\mathbf{R}}_x] \mathbf{T}_{\mathbf{R}_x}(\theta), \quad (20)$$

$$\frac{d\mathbf{T}_{\mathbf{R}_y}(\theta)}{d\theta} = \begin{pmatrix} 0 & 0 & 1 & 0 \\ 0 & 0 & 0 & 0 \\ -1 & 0 & 0 & 0 \\ 0 & 0 & 0 & 0 \end{pmatrix} \mathbf{T}_{\mathbf{R}_y}(\theta) = [\hat{\mathbf{R}}_y] \mathbf{T}_{\mathbf{R}_y}(\theta), \quad (21)$$

$$\frac{d\mathbf{T}_{\mathbf{R}_z}(\theta)}{d\theta} = \begin{pmatrix} 0 & -1 & 0 & 0 \\ 1 & 0 & 0 & 0 \\ 0 & 0 & 0 & 0 \\ 0 & 0 & 0 & 0 \end{pmatrix} \mathbf{T}_{\mathbf{R}_z}(\theta) = [\hat{\mathbf{R}}_z] \mathbf{T}_{\mathbf{R}_z}(\theta), \quad (22)$$

where each of the augmented skew-symmetric matrices  $[\hat{\mathbf{R}}]$  above corresponds to one of the generators of  $\mathbf{SE}(3)$  which lies in  $\mathfrak{se}(3)$ , the tangent space of  $\mathbf{SE}(3)$ . If a joints defined positive rotation is a negative rotation about the axis, as is  $\mathbf{E}_7$  and  $\mathbf{E}_{11}$  in the ETS of the Panda shown in Figure 1, then  $\mathbf{T}_{\mathbf{R}_i}(\theta)^\top$  is used to calculate the derivative.

**Derivative of a Pure Translation** Consider the three elementary translations  $\mathbf{T}_t$  shown in Figure 2.

The derivative of a homogeneous transformation matrix with respect to translation is required when considering a prismatic joint. For an ETS, these translations are embedded in  $\mathbf{SE}(3)$  as  $\mathbf{T}_{t_x}$ ,  $\mathbf{T}_{t_y}$ , and  $\mathbf{T}_{t_z}$  which are pure translations with zero rotational component. We can show that the derivative of each elementary translation with respect to a translation is

$$\frac{d\mathbf{T}_{t_x}(d)}{dd} = \begin{pmatrix} 0 & 0 & 0 & 1 \\ 0 & 0 & 0 & 0 \\ 0 & 0 & 0 & 0 \\ 0 & 0 & 0 & 0 \end{pmatrix} = [\hat{\mathbf{t}}_x], \quad (23)$$

$$\frac{d\mathbf{T}_{t_y}(d)}{dd} = \begin{pmatrix} 0 & 0 & 0 & 0 \\ 0 & 0 & 0 & 1 \\ 0 & 0 & 0 & 0 \\ 0 & 0 & 0 & 0 \end{pmatrix} = [\hat{\mathbf{t}}_y], \quad (24)$$

$$\frac{d\mathbf{T}_{t_z}(d)}{dd} = \begin{pmatrix} 0 & 0 & 0 & 0 \\ 0 & 0 & 0 & 0 \\ 0 & 0 & 0 & 1 \\ 0 & 0 & 0 & 0 \end{pmatrix} = [\hat{\mathbf{t}}_z], \quad (25)$$

where each of the augmented skew symmetric matrices  $[\hat{\mathbf{t}}]$  above are the remaining three generators of  $\mathbf{SE}(3)$  which lie in  $\mathfrak{se}(3)$ . No changes are required if a joints defined positive translation is a negative translation along the axis.

**Figure 4.** Visualisation of a homogeneous transformation matrix (the derivatives share the form of  $\mathbf{T}$ , except will have a 0 instead of a 1 located at  $\mathbf{T}_{44}$ ). Where the matrix  $\rho(\mathbf{T}) \in \mathbb{R}^{3 \times 3}$  of red boxes forms the rotation component, and the vector  $\tau(\mathbf{T}) \in \mathbb{R}^3$  of blue boxes form the translation component. The rotation component can be extracted through the function  $\rho(\cdot) : \mathbb{R}^{4 \times 4} \mapsto \mathbb{R}^{3 \times 3}$ , while the translation component can be extracted through the function  $\tau(\cdot) : \mathbb{R}^{4 \times 4} \mapsto \mathbb{R}^3$ .

## The Manipulator Jacobian

Now we can calculate the derivative of an ETS. To find out how the  $j^{\text{th}}$  joint affects the end-effector pose, apply the chain rule to (1)

$$\begin{aligned} \frac{\partial \mathbf{T}(\mathbf{q})}{\partial q_j} &= \frac{\partial}{\partial q_j} (\mathbf{E}_1(\eta_1) \mathbf{E}_2(\eta_2) \dots \mathbf{E}_M(\eta_M)) \\ &= \prod_{i=1}^{\mu(j)-1} \mathbf{E}_i(\eta_i) \frac{d\mathbf{E}_{\mu(j)}(q_j)}{dq_j} \prod_{i=\mu(j)+1}^M \mathbf{E}_i(\eta_i). \end{aligned} \quad (26)$$

The derivative of the elementary transform with respect to a joint coordinate in (26) is obtained using one of (20), (21), or (22) for a revolute joint, or one of (23), (24), or (25) for a prismatic joint.

Using (13) with (26) we can form the angular velocity component of the  $j^{\text{th}}$  column of the manipulator Jacobian

$$\mathbf{J}_{\omega_j}(\mathbf{q}) = \vee_{\times} \left( \rho \left( \frac{\partial \mathbf{T}(\mathbf{q})}{\partial q_j} \right) \rho(\mathbf{T}(\mathbf{q}))^\top \right) \quad (27)$$

and using (11) with (26), the translational velocity component of the  $j^{\text{th}}$  column of the manipulator Jacobian is

$$\mathbf{J}_{\nu_j}(\mathbf{q}) = \tau \left( \frac{\partial \mathbf{T}(\mathbf{q})}{\partial q_j} \right). \quad (28)$$

Stacking the translational and angular velocity components, the  $j^{\text{th}}$  column of the manipulator Jacobian becomes

$$\mathbf{J}_j(\mathbf{q}) = \begin{pmatrix} \mathbf{J}_{\nu_j}(\mathbf{q}) \\ \mathbf{J}_{\omega_j}(\mathbf{q}) \end{pmatrix} \in \mathbb{R}^6 \quad (29)$$

where the full manipulator Jacobian is

$$\mathbf{J}(\mathbf{q}) = (\mathbf{J}_1(\mathbf{q}) \quad \dots \quad \mathbf{J}_n(\mathbf{q})) \in \mathbb{R}^{6 \times n}. \quad (30)$$

## Fast Manipulator Jacobian

Calculating the manipulator Jacobian using (27) and (28) is easy to understand, but has  $\mathcal{O}(n^2)$  time complexity – we can do better.

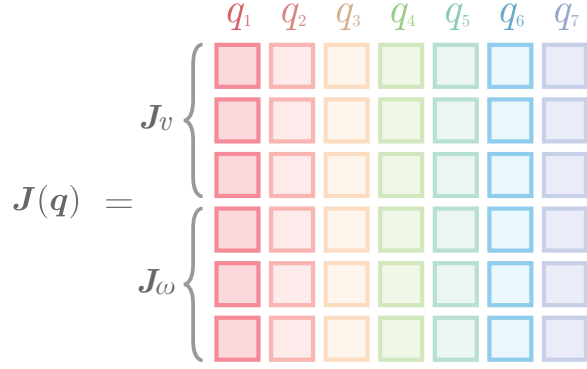


**Figure 5.** Visualisation of the Jacobian  $\mathbf{J}(\mathbf{q})$  of a 7-jointed manipulator. Each column describes how the end-effector pose changes due to motion of the corresponding joint. The top three rows  $\mathbf{J}_v$  correspond to the linear velocity of the end-effector while the bottom three rows  $\mathbf{J}_\omega$  correspond to the angular velocity of the end-effector.

Expanding (27) using (26) and simplifying using  $\mathbf{R}\mathbf{R}^\top = \mathbf{1}$  gives

$$\mathbf{J}_{\omega_j}(\mathbf{q}) = \vee \times \left( \rho({}^0\mathbf{T}_j) \rho([\hat{\mathbf{G}}_{\mu(j)}]) (\rho({}^0\mathbf{T}_j)^\top) \right) \quad (31)$$

where  ${}^0\mathbf{T}_j$  represents the transform from the base frame to joint  $j$  as described by (5), and  $[\hat{\mathbf{G}}_{\mu(j)}]$  corresponds to one of the 6 generators from equations (20)-(22) and (23)-(25).

In the case of a prismatic joint,  $\rho(\hat{\mathbf{G}}_{\mu(j)})$  will be a  $3 \times 3$  matrix of zeros which results in zero angular velocity. In the case of a revolute joint, the angular velocity is parallel to the axis of joint rotation.

$$\mathbf{J}_{\omega_j}(\mathbf{q}) = \begin{cases} \hat{\mathbf{n}}_j & \text{if } \mathbf{E}_m = \mathbf{T}_{\mathbf{R}_x} \\ \hat{\mathbf{o}}_j & \text{if } \mathbf{E}_m = \mathbf{T}_{\mathbf{R}_y} \\ \hat{\mathbf{a}}_j & \text{if } \mathbf{E}_m = \mathbf{T}_{\mathbf{R}_z} \\ (0 \ 0 \ 0)^\top & \text{if } \mathbf{E}_m = \mathbf{T}_t \end{cases} \quad (32)$$

where  $(\hat{\mathbf{n}}_j \ \hat{\mathbf{o}}_j \ \hat{\mathbf{a}}_j) = \rho({}^0\mathbf{T}_j)$  are the columns of a rotation matrix as shown in Figure 6.

Expanding (28) using (26) provides

$$\mathbf{J}_{\nu_j}(\mathbf{q}) = \tau \left( {}^0\mathbf{T}_j [\hat{\mathbf{G}}_{\mu(j)}]^j \mathbf{T}_e \right) \quad (33)$$

which reduces to

$$\mathbf{J}_{\nu_j}(\mathbf{q}) = \begin{cases} \hat{\mathbf{a}}_j y_e - \hat{\mathbf{o}}_j z_e & \text{if } \mathbf{E}_m = \mathbf{T}_{\mathbf{R}_x} \\ \hat{\mathbf{n}}_j z_e - \hat{\mathbf{a}}_j x_e & \text{if } \mathbf{E}_m = \mathbf{T}_{\mathbf{R}_y} \\ \hat{\mathbf{o}}_j x_e - \hat{\mathbf{n}}_j y_e & \text{if } \mathbf{E}_m = \mathbf{T}_{\mathbf{R}_z} \\ \hat{\mathbf{n}}_j & \text{if } \mathbf{E}_m = \mathbf{T}_{t_x} \\ \hat{\mathbf{o}}_j & \text{if } \mathbf{E}_m = \mathbf{T}_{t_y} \\ \hat{\mathbf{a}}_j & \text{if } \mathbf{E}_m = \mathbf{T}_{t_z} \end{cases} \quad (34)$$

where  $(x_e \ y_e \ z_e)^\top = \tau({}^j\mathbf{T}_e)$ .

This simplification reduces the time complexity of computation of the manipulator Jacobian to  $\mathcal{O}(n)$ .

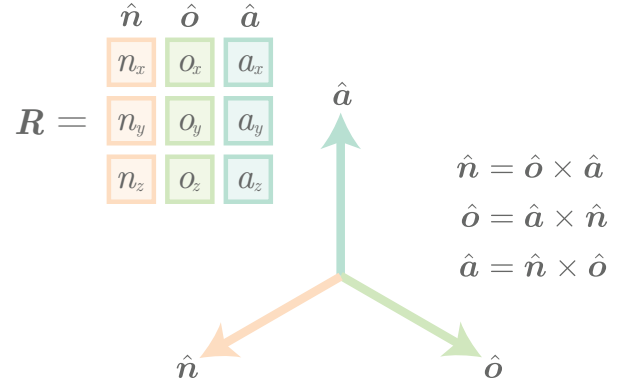


**Figure 6.** The two vector representation of a rotation matrix  $\mathbf{R} \in \text{SO}(3)$ . The rotation matrix  $\mathbf{R}$  describes the coordinate frame in terms of three orthogonal vectors  $\hat{\mathbf{n}}$ ,  $\hat{\mathbf{o}}$ , and  $\hat{\mathbf{a}}$  which are the axes of the rotated frame expressed in the reference coordinate frame  $\hat{\mathbf{x}}$ ,  $\hat{\mathbf{y}}$ , and  $\hat{\mathbf{z}}$ . As shown above, each of the vectors  $\hat{\mathbf{n}}$ ,  $\hat{\mathbf{o}}$ , and  $\hat{\mathbf{a}}$  can be calculated using the cross product of the other two.

## Manipulator Jacobian Applications

The manipulator Jacobian is widely used in robotic control algorithms and the remainder of this article details several applications of the manipulator Jacobian.

### Resolved-Rate Motion Control

Resolved-rate motion control (RRMC) is a simple and elegant method to generate straight-line motion of the end effector [5]. While useful in its own right, RRMC lays the foundations for numerical inverse kinematics [6], [7], and reactive motion controllers [8]–[12]. RRMC is a direct application of the first-order differential equation we generated in (17).

We first re-arrange (17)

$$\dot{\mathbf{q}} = {}^0\mathbf{J}(\mathbf{q})^{-1} {}^0\boldsymbol{\nu} \quad (35)$$

which can only be solved when  $\mathbf{J}(\mathbf{q})$  is square (and non-singular), which is when the robot has 6 degrees-of-freedom.

For redundant robots there is no unique solution for (35). Consequently, the most common approach is to use the Moore-Penrose pseudoinverse

$$\dot{\mathbf{q}} = {}^0\mathbf{J}(\mathbf{q})^+ {}^0\boldsymbol{\nu}. \quad (36)$$

The pseudoinverse will return joint velocities with the minimum velocity norm of the possible solutions.

Immediately from this, we can construct a primitive open-loop velocity controller. At each time step we must calculate the manipulator Jacobian  $\mathbf{J}(\mathbf{q})$  which is a function of the robot's current configuration  $\mathbf{q}$ . Then we set  $\boldsymbol{\nu}$  to the desired spatial velocity of the end-effector.

A more useful application of RRMC is to employ it in a closed-loop pose controller which we denote position-based servoing (PBS). Using this method we can get the end-effector to travel in a straight line, in the robot's task space, towards some desired end-effector pose as displayed in Figure 7. The PBS scheme relies on an error vector which represents the translation and rotation from the end-effector's current pose to the desired pose

$$\mathbf{e} = \begin{pmatrix} \tau({}^0\mathbf{T}_{e^*}) - \tau({}^0\mathbf{T}_e) \\ \alpha(\rho({}^0\mathbf{T}_{e^*})\rho({}^0\mathbf{T}_e)^\top) \end{pmatrix} \in \mathbb{R}^6 \quad (37)$$

where the top three rows correspond to the translational error in the world frame, the bottom three rows correspond to the rotational error in the world frame,  ${}^0\mathbf{T}_e$  is the forward kinematics of the robot which represents the end-effector pose in the base frame of the robot,  ${}^0\mathbf{T}_{e^*}$  is the desired end-effector pose in the base frame of the robot (\* denotes desired not actual), and  $\alpha(\cdot) : \mathbf{SO}(3) \mapsto \mathbb{R}^3$  transforms a rotation matrix to its Euler vector equivalent [7].

Using the numbering convention from Figure 6 we define  $\rho(\mathbf{T}) = \mathbf{R} = \{r_{ij}\}$  and

$$\mathbf{l} = \begin{pmatrix} r_{32} - r_{23} \\ r_{13} - r_{31} \\ r_{21} - r_{12} \end{pmatrix}. \quad (38)$$

If  $\mathbf{R}$  is not a diagonal matrix then the angle-axis equivalent of  $\mathbf{R}$  is calculated as

$$\alpha(\mathbf{R}) = \frac{\text{atan2}(\|\mathbf{l}\|, r_{11} + r_{22} + r_{33} - 1)}{\|\mathbf{l}\|} \mathbf{l}. \quad (39)$$

If  $\mathbf{R}$  is a diagonal matrix then we use different formulas. For the case where  $(r_{11} \ r_{22} \ r_{33}) = (1 \ 1 \ 1)$  then

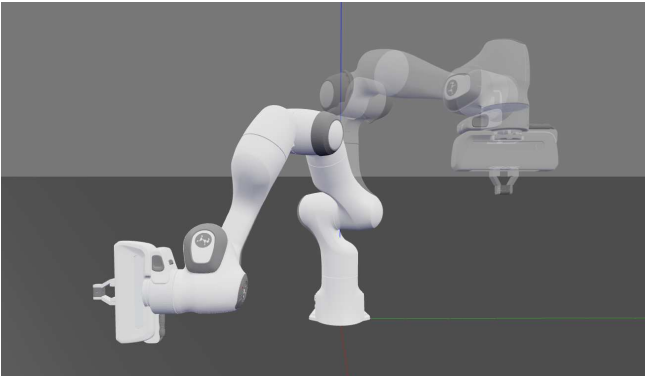


**Figure 7.** Visualisation of a Panda robot which has been controlled by a position based servoing control scheme utilising resolved-rate motion control. The end-effectors pose has both translated and rotated to reach the desired pose.

$$\alpha(\mathbf{R}) = (0 \ 0 \ 0)^\top \text{ otherwise}$$

$$\alpha(\mathbf{R}) = \frac{\pi}{2} \begin{pmatrix} r_{11} + 1 \\ r_{22} + 1 \\ r_{33} + 1 \end{pmatrix}. \quad (40)$$

To construct the PBS scheme we take the error term from (37) to set  $\boldsymbol{\nu}$  in (35) (or (36) for robots with 7+ degrees of freedom) at each time step

$$\boldsymbol{\nu} = k\mathbf{e} \quad (41)$$

where  $k$  is a proportional gain term which controls the rate of convergence to the goal. It is important to remember that the vector  $\mathbf{e}$  is non-homogeneous since its elements have different units (metres and radians).  $k$  is typically a diagonal matrix to set gains for each task-space DoF

$$\mathbf{k} = \text{diag}(k_t, k_t, k_t, k_r, k_r, k_r) \quad (42)$$

where  $k_t$  is the translational motion gain and  $k_r$  is the rotational motion gain. Note that since the error  $\mathbf{e}$  is in the base-frame of the robot we must use the base-frame manipulator Jacobian  ${}^0\mathbf{J}(\mathbf{q})$  in (35) or (36).

The control scheme we have just described will cause the error to asymptotically decrease to zero. For real applications this is slow and impractical. We can improve this by increasing  $k_t$  and  $k_r$  and capping the  $\boldsymbol{\nu}$  norm at some value  $\nu_m$ , before stopping when the error norm drops below some value  $\|\mathbf{e}\|_m$

$$\boldsymbol{\nu} = \begin{cases} k\mathbf{e} \frac{\nu_m}{\|k\mathbf{e}\|} & \text{if } \|k\mathbf{e}\| > \nu_m \\ k\mathbf{e} & \text{if } \nu_m \geq \|k\mathbf{e}\| > \|\mathbf{e}\|_m \\ \mathbf{0} & \text{otherwise.} \end{cases} \quad (43)$$

This will cause the error to reduce at a consistent rate until the end of the motion where the velocity asymptotically decreases to safely stop the robot. The effect of

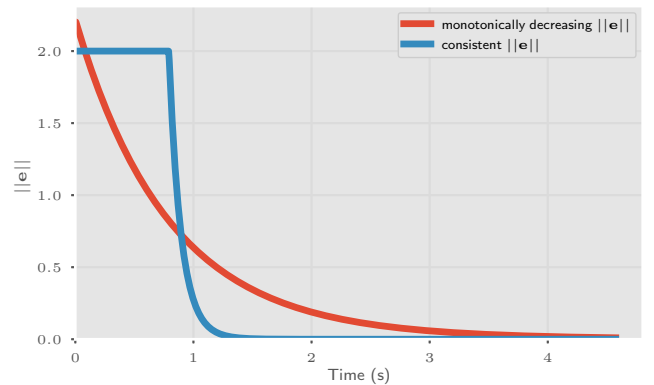


**Figure 8.** Comparison of the Euclidean distance error from the end-effectors pose to the desired pose using two different strategies.

this is displayed in Figure 8. Alternatively, (43) could be modified to create different velocity profiles, such as a linearly decreasing velocity norm, if desired. Additionally, (43) can be modified to adjust the translational and angular velocity profiles separately.

## Numerical Inverse Kinematics

Inverse kinematics deals is the problem of determining the corresponding joint coordinates, given some end-effector pose. There are two approaches to solving inverse kinematics: analytical and numerical.

Analytical formulas must be pre-generated for a given manipulator and in some cases may not exist. The IK-Fast program, provided as a part of OpenRAVE, pre-compiles analytic solutions for a given manipulator in optimised C++ code [13]. After this initial step, inverse kinematics can be computed rapidly, taking as little as 5 microseconds. However, analytic solutions generally cannot optimise for additionally criteria such as joint limits.

Numerical inverse kinematics use an iterative technique and can additionally consider extra constraints such as collision avoidance, joint limit avoidance, or manipulability [6], [7], [14]. In this section we first construct a primitive numerical inverse kinematics solver, before showing how it can be improved using advanced optimisation techniques.

The Newton-Raphson (NR) method for inverse kinematics is remarkably similar to RRMC in a position-based servoing scheme. However, instead of sending joint velocities to the robot, the *joint velocities* update the configuration of the manipulator until the goal pose is reached. To find the joint coordinates which correspond to some end-effector pose  ${}^0\mathbf{T}_{e^*}$ , the NR method seeks to minimise an error function

$$E = \frac{1}{2} \mathbf{e}^\top \mathbf{W}_e \mathbf{e} \quad (44)$$

where  $\mathbf{e}$  is defined in (36), and  $\mathbf{W}_e = \text{diag}(\mathbf{w}_e)$  ( $\mathbf{w}_e \in \mathbb{R}_{>0}^n$ ) is a diagonal weighting matrix which prioritises the corresponding error term. To achieve this, we iterate upon the following

$$\mathbf{q}_{k+1} = \mathbf{q}_k + {}^0\mathbf{J}(\mathbf{q}_k)^{-1} \mathbf{e}_k. \quad (45)$$

When using the NR method, the initial joint coordinates  $\mathbf{q}_0$ , should correspond to a non-singular manipulator pose, since it uses the manipulator Jacobian. When the problem is solvable, it converges very quickly. However, this method frequently fails to converge on the goal. We can improve the solvability of the problem by using the Gauss-Newton (GN) method

$$\mathbf{q}_{k+1} = \mathbf{q}_k + \left( \mathbf{J}(\mathbf{q}_k)^\top \mathbf{W}_e \mathbf{J}(\mathbf{q}_k) \right)^{-1} \mathbf{g}_k \quad (46)$$

$$\mathbf{g}_k = \mathbf{J}(\mathbf{q}_k)^\top \mathbf{W}_e \mathbf{e}_k \quad (47)$$

where  $\mathbf{J} = {}^0\mathbf{J}$  is the base-frame manipulator Jacobian. If  $\mathbf{J}(\mathbf{q}_k)$  is non-singular, and  $\mathbf{W}_e = \mathbf{1}_n$ , then (46) provides the pseudoinverse solution to (45). However, if  $\mathbf{J}(\mathbf{q}_k)$  is singular, (46) can not be computed and the GN solution is infeasible.

Most linear algebra libraries (including the Python numpy library) implement the pseudoinverse using singular value decomposition, which is robust to singular matrices. Therefore, we can make both solvers more robust by using the pseudoinverse instead of the normal inverse in (45) and (46).

However, the computation is still unstable near singular points. We can further improve the solvability through the Levenberg-Marquardt (LM) method

$$\mathbf{q}_{k+1} = \mathbf{q}_k + (\mathbf{A}_k)^{-1} \mathbf{g}_k \quad (48)$$

$$\mathbf{A}_k = \mathbf{J}(\mathbf{q}_k)^\top \mathbf{W}_e \mathbf{J}(\mathbf{q}_k) + \mathbf{W}_n \quad (49)$$

where  $\mathbf{W}_n = \text{diag}(\mathbf{w}_n)$  ( $\mathbf{w}_n \in \mathbb{R}_{>0}^n$ ) is a diagonal damping matrix. The damping matrix ensures that  $\mathbf{A}_k$  is non-singular and positive definite. The performance of the LM method largely depends on the choice of  $\mathbf{W}_n$ . Wampler [15] proposed  $\mathbf{w}_n$  to be a constant, Chan and Lawrence [16] proposed a damped least-squares method with

$$\mathbf{W}_n = \lambda E_k \mathbf{1}_n \quad (50)$$

where  $\lambda$  is a constant which does not have much influence on performance. Sugihara [7] proposed

$$\mathbf{W}_n = E_k \mathbf{1}_n + \text{diag}(\tilde{\mathbf{w}}_n) \quad (51)$$

where  $\tilde{\mathbf{w}}_n \in \mathbb{R}^n$ ,  $\hat{w}_{n_i} = l^2 \sim 0.01l^2$ , and  $l$  is the length of a typical link within the manipulator.

An important point to note is that the above methods are subject to local minima and in some cases will fail to converge on the solution. The choice of the initial joint configuration  $\mathbf{q}_0$  is important. An alternative approach is to re-start an IK problem with a new random  $\mathbf{q}_0$  after a few 20 ~ 50 iterations rather than persist with a single attempt with 500 ~ 5000 iterations. This is a simple but effective method of performing a global search for the IK solution.

We display a comparison of IK methods presented in this Tutorial in Table 1. Table 1 shows results for several IK algorithms trying to solve for 10 000 randomly generated reachable end-effector poses using a 6 degree-of-freedom UR5 manipulator. We show each method initialised with a random valid  $\mathbf{q}_0$  and a maximum of 500 iterations to reach the goal before being declared infeasible. We also show methods (denoted with the  $g$  subscript) with 100 searches to reach to the goal where a new search is initialised with a new random valid  $\mathbf{q}_0$  after 30 iterations. The iterations recorded for this method include the iterations from failed searches.



**Table 1.** Numerical IK Methods Compared over 10000 Problems on a UR5 Manipulator

Method	Searches Allowed	Iter. Allowed	Mean Iter.	Median Iter.	Infeasible Count	Infeasible %	Mean Searches	Max Searches
NR	1	500	21.34	16.0	1093	10.93%	1.0	1.0
GN	1	500	21.6	16.0	1078	10.78%	1.0	1.0
NR Pseudoinverse	1	500	21.24	16.0	1100	11.0%	1.0	1.0
GN Pseudoinverse	1	500	21.72	16.0	1090	10.9%	1.0	1.0
LM (Wampler $\lambda = 1e-4$ )	1	500	20.1	14.0	934	9.34%	1.0	1.0
LM (Wampler $\lambda = 1e-6$ )	1	500	29.84	17.0	529	5.29%	1.0	1.0
LM (Chan $\lambda=1.0$ )	1	500	16.58	14.0	1011	10.11%	1.0	1.0
LM (Chan $\lambda=0.1$ )	1	500	9.43	9.0	963	9.63%	1.0	1.0
LM (Sugihara $w_n = 1e-3$ )	1	500	20.54	15.0	1024	10.24%	1.0	1.0
LM (Sugihara $w_n = 1e-4$ )	1	500	17.01	14.0	1011	10.11%	1.0	1.0
NR	100	30	30.16	18.0	0	0.0%	1.47	25.0
GN	100	30	30.33	18.0	0	0.0%	1.48	23.0
NR Pseudoinverse	100	30	30.27	18.0	0	0.0%	1.47	20.0
GN Pseudoinverse	100	30	30.65	18.0	0	0.0%	1.49	20.0
LM (Wampler $\lambda = 1e-4$ )	100	30	25.23	15.0	0	0.0%	1.35	17.0
LM (Wampler $\lambda = 1e-6$ )	100	30	29.3	18.0	0	0.0%	1.45	24.0
LM (Chan $\lambda=1.0$ )	100	30	22.6	15.0	0	0.0%	1.25	18.0
LM (Chan $\lambda=0.1$ )	100	30	15.33	9.0	0	0.0%	1.2	18.0
LM (Sugihara $w_n = 1e-3$ )	100	30	26.49	16.0	0	0.0%	1.35	18.0
LM (Sugihara $w_n = 1e-4$ )	100	30	23.04	15.0	0	0.0%	1.26	18.0

We have presented some useful IK methods but it is by no means an exhaustive list. Sugihara [7] provides a good comparison of many different numerical IK methods. In Part II of this tutorial we explore advanced IK techniques which incorporate additional constraints into the optimisation.

## Manipulator Performance Metrics

Manipulator performance metrics seek to quantify the performance of a manipulator in a given configuration. In this section, we explore two common manipulator performance metrics based on the manipulator Jacobian. A full survey of performance metrics can be found in [17]. It is important to note several considerations on how manipulator-based performance metrics should be used in practice. Firstly, the metrics are unitless, and the upper bound of a metric depends on the manipulator kinematic model (i.e. joint types and link lengths). Consequently, metrics computed for different manipulators are not directly comparable. Secondly, the manipulator Jacobian contains three rows corresponding to translational rates, and three rows corresponding to angular rates. Therefore, any metric using the whole Jacobian will produce a non-homogeneous result due to the mixed

units. Depending on the manipulator scale, this can cause either the translational or rotational component to dominate the result. This problem also arises in manipulators with mixed prismatic and revolute joints. In general, the most intuitive use of performance metrics comes from using only the translational or rotational rows of the manipulator Jacobian (where the choice of which depends on the use case), and only using the metric on a manipulator comprising a single joint type [17].

**Manipulability Index** The Yoshikawa manipulability index [18] is the most widely used and accepted performance metric [17]. The index is calculated as

$$m(\mathbf{q}) = \sqrt{\det(\hat{\mathbf{J}}(\mathbf{q})\hat{\mathbf{J}}(\mathbf{q})^\top)} \quad (52)$$

where  $\hat{\mathbf{J}}(\mathbf{q}) \in \mathbb{R}^{3 \times n}$  is either the translational or rotational rows of  $\mathbf{J}(\mathbf{q})$  causing  $m(\mathbf{q})$  to describe the corresponding component of manipulability. Note that Yoshikawa used  $\mathbf{J}(\mathbf{q})$  instead of  $\hat{\mathbf{J}}(\mathbf{q})$  in (52) but we describe it so due to limitations of Jacobian based measures previously discussed. The scalar  $m(\mathbf{q})$  describes the volume of a 3-dimensional ellipsoid – if this ellipsoid is close to spherical, then the manipulator can achieve any arbitrary end-effector (translational or rotational depending

on  $\hat{\mathbf{J}}(\mathbf{q})$  velocity. The ellipsoid is described by three radii aligned with its principal axes. A small radius indicates the robot’s inability to achieve a velocity in the corresponding direction. At a singularity, the ellipsoid’s radius becomes zero along the corresponding axis and the volume becomes zero. If the manipulator’s configuration is well conditioned, these ellipsoids will have a larger volume. Therefore, the manipulability index is essentially a measure of how easily a manipulator can achieve an arbitrary velocity.

**Condition Number** The condition number of the manipulator Jacobian was proposed as a performance measure in [19]. The condition number is

$$\kappa = \frac{\sigma_{\max}}{\sigma_{\min}} \in [1, \infty] \quad (53)$$

where  $\sigma_{\max}$  and  $\sigma_{\min}$  are the maximum and minimum singular values of  $\hat{\mathbf{J}}(\mathbf{q})$  respectively. The condition number is a measure of velocity isotropy. A condition number close to 1 means that the manipulator can achieve a velocity in a direction equally as easily as any other direction. However, a high condition number does not guarantee a high manipulability index where the manipulator may struggle to move in all directions.

## Acknowledgments

We acknowledge the continued support from Queensland University of Technology Centre for Robotics (QCR). We would also like to thank the members of QCR who have provided valuable feedback and insights while testing this tutorial and associated Jupyter Notebooks.

## Conclusions

In Part 1 of this tutorial we have covered foundational aspects of manipulator differential kinematics. We first detailed a procedure for describing the kinematics of any manipulator and used this model to derive formulas for calculating the forward and first-order differential kinematics. We then detailed some applications unlocked by these formulas, including reactive motion control, inverse kinematics and methods which describe the performance of a manipulator at a given configuration. In Part II, we explore second-order differential kinematics and detail how it can improve applications detailed in Part 1 while also unlocking new applications.

## References

- [1] P. Corke and J. Haviland, “Not your grandmother’s toolbox—the robotics toolbox reinvented for Python,” in *2021 IEEE international conference on robotics and automation (ICRA)*, IEEE, 2021.

- [2] P. I. Corke, “A simple and systematic approach to assigning Denavit–Hartenberg parameters,” *IEEE transactions on robotics*, vol. 23, no. 3, pp. 590–594, 2007.
- [3] R. S. Hartenberg and J. Denavit, “A kinematic notation for lower pair mechanisms based on matrices,” 1955.
- [4] P. Corke, *Robotics, Vision and Control*, 2nd ed. Springer International Publishing, 2017.
- [5] D. E. Whitney, “Resolved motion rate control of manipulators and human prostheses,” *IEEE Transactions on Man-Machine Systems*, vol. 10, no. 2, pp. 47–53, 1969.
- [6] Pyung Chang, “A closed-form solution for inverse kinematics of robot manipulators with redundancy,” *IEEE Journal on Robotics and Automation*, vol. 3, no. 5, pp. 393–403, 1987.
- [7] T. Sugihara, “Solvability-unconcerned inverse kinematics by the levenberg–marquardt method,” *IEEE Transactions on Robotics*, vol. 27, no. 5, pp. 984–991, 2011.
- [8] J. Haviland and P. Corke, “Maximising manipulability during resolved-rate motion control,” *arXiv preprint arXiv:2002.11901*, 2020.
- [9] D. Guo and Y. Zhang, “Acceleration-level inequality-based MAN scheme for obstacle avoidance of redundant robot manipulators,” *IEEE Transactions on Industrial Electronics*, vol. 61, no. 12, pp. 6903–6914, Dec. 2014.
- [10] J. Haviland and P. Corke, “NEO: A novel expeditious optimisation algorithm for reactive motion control of manipulators,” *IEEE Robotics and Automation Letters*, 2021.
- [11] O. Khatib, “Real-time obstacle avoidance for manipulators and mobile robots,” in *Autonomous robot vehicles*, Springer, 1986, pp. 396–404.
- [12] D.-H. Park, H. Hoffmann, P. Pastor, and S. Schaal, “Movement reproduction and obstacle avoidance with dynamic movement primitives and potential fields,” in *IEEE International Conference on Humanoid Robots*, 2008.
- [13] R. Diankov, “Automated construction of robotic manipulation programs,” Ph.D. dissertation, Carnegie Mellon University, Robotics Institute, Aug. 2010.
- [14] A. S. Deo and I. D. Walker, “Adaptive non-linear least squares for inverse kinematics,” in *[1993] Proceedings IEEE International Conference on Robotics and Automation*, IEEE, 1993, pp. 186–193.
- [15] C. W. Wampler, “Manipulator inverse kinematic solutions based on vector formulations and damped least-squares methods,” *IEEE Transactions on Systems, Man, and Cybernetics*, vol. 16, no. 1, pp. 93–101, 1986.
- [16] S. K. Chan and P. D. Lawrence, “General inverse kinematics with the error damped pseudoinverse,” in *Proceedings. 1988 IEEE international conference on robotics and automation*, IEEE, 1988, pp. 834–839.
- [17] S. Patel and T. Sobh, “Manipulator performance measures—a comprehensive literature survey,” *Journal of Intelligent & Robotic Systems*, vol. 77, no. 3, pp. 547–570, 2015.
- [18] T. Yoshikawa, “Manipulability of Robotic Mechanisms,” *The International Journal of Robotics Research*, vol. 4, no. 2, pp. 3–9, 1985.
- [19] J. K. Salisbury and J. J. Craig, “Articulated hands: Force control and kinematic issues,” *The International journal of Robotics research*, vol. 1, no. 1, pp. 4–17, 1982.